

Insight into Graphite Oxidation in a NiO-based Hybrid Direct Carbon Fuel Cell

Cairong Jiang^{ab}, Can Cui^a, Jianjun Ma^{ab*}, and John T. S. Irvine^c

a, School of Materials Science and Engineering, Sichuan University of Science and Engineering, Zigong, Sichuan, 643000, P. R. China

b, Material Corrosion and Protection Key Laboratory of Sichuan province, Zigong, Sichuan, 643000, P. R. China

c, School of Chemistry, University of St Andrews, KY16 9ST, Scotland, United Kingdom

**Corresponding author: JM: Email: jjma@suse.edu.cn or majianjun@mail.ustc.edu.cn*

Abstract:

A direct carbon fuel cell is an electricity generation device using solid carbon as a fuel directly with no reforming process. In this study, three-carbon fuels, graphitic carbon (GC), carbon black (CB), and biomass carbon (BC) are tested as the fuel to investigate the influence of carbon fuel properties on the cell performance in HDCFC with a traditional nickel oxide as the anode. Either an electrolyte-supported cell with a thin nickel oxide anode or an anode-supported cell with a thick nickel oxide anode is used to evaluate the electrochemical reactivity of carbon samples. These three-carbon fuels are characterised on the crystal structure, particle size, composition, and surface property. It is found that GC shows excellent cell performance on thin nickel oxide anode. However, it displays relatively slow electrochemical reactivity on the thick anode due to its great extent of carbon oxidation. BC shows good initial cell performance but fast degradation of the cell performance, as much more hydrogen is released at the beginning of the cell test. The anode reactions of HDCFCs are explored by the in-situ gas analysis in open circuits and under current load conditions. It is observed that GC produces the highest amount of CO among these three fuels, suggesting that carbon oxidation is the dominant electrochemical process in HDCFCs after a certain time when most of the hydrogen is released from the pyrolysis process.

Key words: Graphite; Carbon fuel properties; Electrochemical oxidation; In-situ gas analysis

1. Introduction

A direct carbon fuel cell is a device that converts the chemical energy of solid carbon into electricity with no external gasification or reforming process [1-3]. In recent years, it receives more attention due to high energy conversion efficiency and its easy availability of the fuel. Solid carbon can be obtained from a variety of natural resources, e. g., forest, agriculture, and food waste [4]. Up to now, so many kinds of carbon fuels have been applied in DCFCs. Researchers have focused on the investigation of the utility of different fuels like pure carbon [5-8], biochar, coal or even raw biomass in a variety of cell configurations, such as molten hydroxides-based DCFCs, molten carbonates-based DCFCs, and solid oxide conductors DCFCs [9-11].

In hydroxide-based DCFC, Hackett *et al.*[12] evaluated various carbonaceous materials, especially graphite (GC). They investigated the effect of GC rods' fuel structure on the open-circuit voltage and life, and, they also conducted a lifetime comparison.

Weaver *et al.*[13] presented a molten carbonate electrolyte to be used for direct carbon conversion in 1979. They tested several types of carbon fuels and concluded that devolatilised coal is more reactive than spectroscopic carbon and pyrolytic GC. They linked the high reactivity to the large surface area and the poor crystallisation. The most reactive material, JPL coal, produced 100 mA cm^{-2} at 0.8 V vs. reference electrode at 700 °C, the potential at 100 mA cm^{-2} increasing to 0.9 V at 800 °C. Besides, they measured the anode off-gas as 90% CO_2 at a high current density and found the CO_2 / CO ratio decreased at lower current densities. In molten carbonate-based DCFCs, the pore volume and the surface area influence the wettability between the fuel and the molten carbonate, promoting electrochemical reactions in the DCFC system [14]. Chen *et al.*[15] and Peng *et al.* [16] have demonstrated that the wetting behaviour of the carbon anode may be as crucial as the molecular mechanism for carbon oxidation in molten carbon DCFCs. Li *et al.* [17] and co-workers investigated the effects of the chemical and physical properties of fuels such as composition, structure, surface area, and surface functional groups on electrochemical reactions. They found that desirable structure of the carbon fuel for carbonate-based DCFC is to have a high mesoporous surface area and oxygen-rich surface groups [18]. They confirmed that carbon with oxygen-rich surface groups possesses high electrochemical reactivity. They also performed surface modification of activated carbon and carbon particles with acid or air plasma. Similarly, the acid-treated carbon gives the best performance due to the most considerable degree of surface oxygen functional groups [19]. However, Cherepy *et al.*[20]

carried out recently a work using eutectic molten carbonate electrolyte for the direct conversion of solid carbon particulates. They found that the surface area has no substantial effects on the carbon discharge rate.

In recent years, significant efforts have been made to study the relationship between the characteristics of the carbon fuel and the performance of the DCFC device [21-23]. Carbon fuel properties are vitally important to the output performance of direct carbon fuel cells (DCFCs). Features such as surface functional groups, surface area, pore structure, the degree of crystallinity have been investigated, and the effects of these parameters on the cell performance have been evaluated.[6] Although the utilisation of carbon in fuel cells has been widely studied, the oxidation mechanism of carbon at the anode is not fully understood. GC is a typical fuel for DCFCs as its graphitic structure. A literature survey demonstrates that GC has been extensively studied and experimentally evaluated as a fuel in a variety of DCFC configurations. In different settings, the carbon oxidation mechanism might change remarkably. Thus, different conclusions were reported. It is said that carbon fuels with a high surface area (e.g., devolatilised coal) are more accessible to the anode reaction than GC.[13] However, Cherepy *et al.*[20] experimented with various carbon samples in a molten carbonate electrolyte and obtained the best performance of 50 mA cm^{-2} at 0.8 V on GC carbon, which might be due to its excellent conductivity. Vutetakis *et al.* [24] reported GC-fuelled molten carbonate-based DCFCs shows better performance than that of an anthracite-fuelled DCFC, but poorer performance than that of a diamond-fuelled DCFC. Li *et al.*[18] carried out a comparative experiment on GC, carbon black, and active carbon in molten carbonate-DCFCs. In their research, GC showed the lowest electrochemical reactivity at different potentials and temperatures, and the peak power density delivered was around 17 mW cm^{-2} at $800 \text{ }^\circ\text{C}$, implying low electrochemical activity of the highly ordered GC. Recently, Chen *et al.* [25] studied the performance of GC as a fuel in DCFC based molten carbonate $\text{Li}_2\text{CO}_3/\text{K}_2\text{CO}_3/\text{Al}_2\text{O}_3$. They concluded that GC alone could not perform well as the anode fuel in DCFC although it has a regular structure, a high electrical conductivity, and a low resistance. Meanwhile, the influence of GC fuel on the performance and lifetime of the DCFC are still up for debate. From the above results, we can see that most research is focused on the molten carbonate DCFCs. The reactivities of GC in hybrid direct carbon fuel cells with a molten carbonate fuel cell and a solid oxide fuel cell is not extensively studied.

We have demonstrated the carbon oxidation process in a hybrid direct carbon fuel cell using carbon black as fuel in our previous research [26]. Our initial investigation on the application of different carbon

fuels in HDCFCs showed that GC in an anode-supported cell exhibited poor cell performance of 75 mW cm^{-2} , which is much lower than 100 and 210 mW cm^{-2} at $750 \text{ }^\circ\text{C}$ with carbon black and activated carbon as the fuel, respectively [27]. Among all the fuels, biomass carbon (BC, pyrolysed medium density fibreboard) generated the best cell performance with a maximum power density of 878 mW cm^{-2} at $750 \text{ }^\circ\text{C}$ [28].

In this study, we will carry out further investigation on the key factors affecting the electrochemical reactivity of carbon fuels in the HDCFC system. We will focus on the GC fuel on a thin NiO-electrode and a thick NiO-anode. A standard fuel of carbon black (CB) widely used in other literature and a biomass carbon (BC) [29] are used for comparison regarding the difference in chemical and surface properties. In this paper, for the first time, we investigated the electrochemical oxidation of fuel in the DCFC with in-situ gas analysis under electrochemical test.

2. Experimental

2.1 Pre-treatment of carbon fuels

The carbon fuels for experiments are graphite carbon (GC, Cabot), carbon black (CB, XC-72R, Cabot), and biomass carbon (BC). The biomass carbon was pyrolysed at $400 \text{ }^\circ\text{C}$ in nitrogen. A mixture of 62 mol% lithium carbonate (Aldrich Chemical Co., WI, USA) and 38 mol% potassium carbonate (Fisher, UK) was pre-mixed by ball milling in acetone for 24h before mixed with different carbons. The weight ratio of carbon to Li_2CO_3 - K_2CO_3 is 4:1. The same process was used for the carbon-carbonate mixture, followed by drying in the oven at $80 \text{ }^\circ\text{C}$ for overnight.

2.2 Cells preparation and electrochemical characteristics

Electrolyte-supported SOFCs have a configuration of NiO-YSZ layer/YSZ(1 mm)/LSM-YSZ layer. First, a YSZ disk was made by dry pressing and sintering at $1500 \text{ }^\circ\text{C}$ for 10 hrs. Secondly, an anode layer with a mixture of NiO and YSZ in a weight ratio of 60 to 40 was screen printed on one side of the YSZ disk and calcined at $1350 \text{ }^\circ\text{C}$ for 2hrs. Thirdly, a composite cathode layer of $(\text{La}_{0.8}\text{Sr}_{0.2})_{0.95}\text{MnO}_{3-\delta}$ -YSZ was screen printed on the other side of the YSZ disk and calcined at $1100 \text{ }^\circ\text{C}$ for 2hrs. The diameter of the YSZ disk was 20 mm. The diameter of the anode and the cathode was the same, which was 12 mm. The as-prepared cell was painted with silver paste on the anode and the cathode as the current collectors followed by calcined at $800 \text{ }^\circ\text{C}$ for 1hr.

Anode-supported SOFCs have a configuration of NiO-YSZ (1 mm)/ YSZ thin film (5-10 μm)/LSM-

YSZ layer. First, the anode substrate of nickel oxide (Aldrich, 325 mesh) and YSZ (Tosoh, TZ-8Y) with a weight ratio of 60 to 40 was mixed by ball milling for 24 hrs and pressed into a disk with ~1 mm thickness. The slurry of YSZ was obtained by mixing YSZ powder with organic solutions, binders, and plastics for 20 hrs. After that the YSZ slurry was coated onto the pre-calcined anode substrate, the half-cell with the anode substrate and the thin YSZ electrolyte was sintered at 1350 °C for 5 hrs. The thickness of the YSZ electrolyte can be controlled by the slurry concentration, and in the present study, it was 5-10 µm. A cathode of either $(\text{La}_{0.8}\text{Sr}_{0.2})_{0.95}\text{MnO}_{3.5}$ (LSM)-YSZ was screen printed on the surface of the YSZ electrolyte, by calcining at 1100 °C for 2 hrs. The cathode area of the anode-supported cell was the same as the cathode for the electrolyte-supported cell. Finally, the as-prepared cell in ~20 mm diameter was painted with silver paste, pre-calcined at 800 °C for 1 hr, on both sides of the anode and the cathode.

Either an electrolyte-supported cell or an anode-supported cell was sealed on the alumina tube using sealant (Aremco 552), with the anode side up. 2 g mixture of carbon-carbonate (4:1) was weighed and filled into the anode chamber. The purge gas of N_2 was controlled by the valves, and the flow rate of gas was 20 ml/min. The cell performance was measured on Solartron 1280B with 10 mV ac disturbed for AC impedance and 20 mV/step to scan current-voltage curves.

2.3 Sample analysis

The gas analysis was performed on a 3000 micro-Gas Chromatograph equipped with two capillary columns and a backflush injector. A 320 µm×10 m MolSieve column with argon as the carrier gas, was used for hydrogen, nitrogen, carbon monoxide, and methane detection. A 320 µm×8 m PlotU column equipped with a helium carrier gas for carbon dioxide detection. Injection occurred through a backflush injector operated at 110 °C. The separation occurred at 100 °C and 60 °C with a pressure of 30 psi a for MolSieve column and Plot column, respectively. In long-term tests the percentages of gas output were determined, these were converted to gas volumes using the nitrogen purge gas as an internal standard. As the gas content is slightly overestimated the amount of carbon produced over long-term tests, these were then normalised against the total amount of carbon utilised.

The X-ray diffraction (XRD) patterns of carbon samples were recorded on a PANalytical Empyrean Reflection Diffractometer with Cu K α radiation ($\lambda = 1.5418 \text{ \AA}$) using settings of 40 mA and 40 kV, 2 θ range of 10-90 °, step size of 0.02 ° and scan step time of 2 s. A Fourier Transform Infrared spectrophotometer (FTIR; Shimadzu, IRAffinity-1S) was used for the FTIR spectra measurements. The

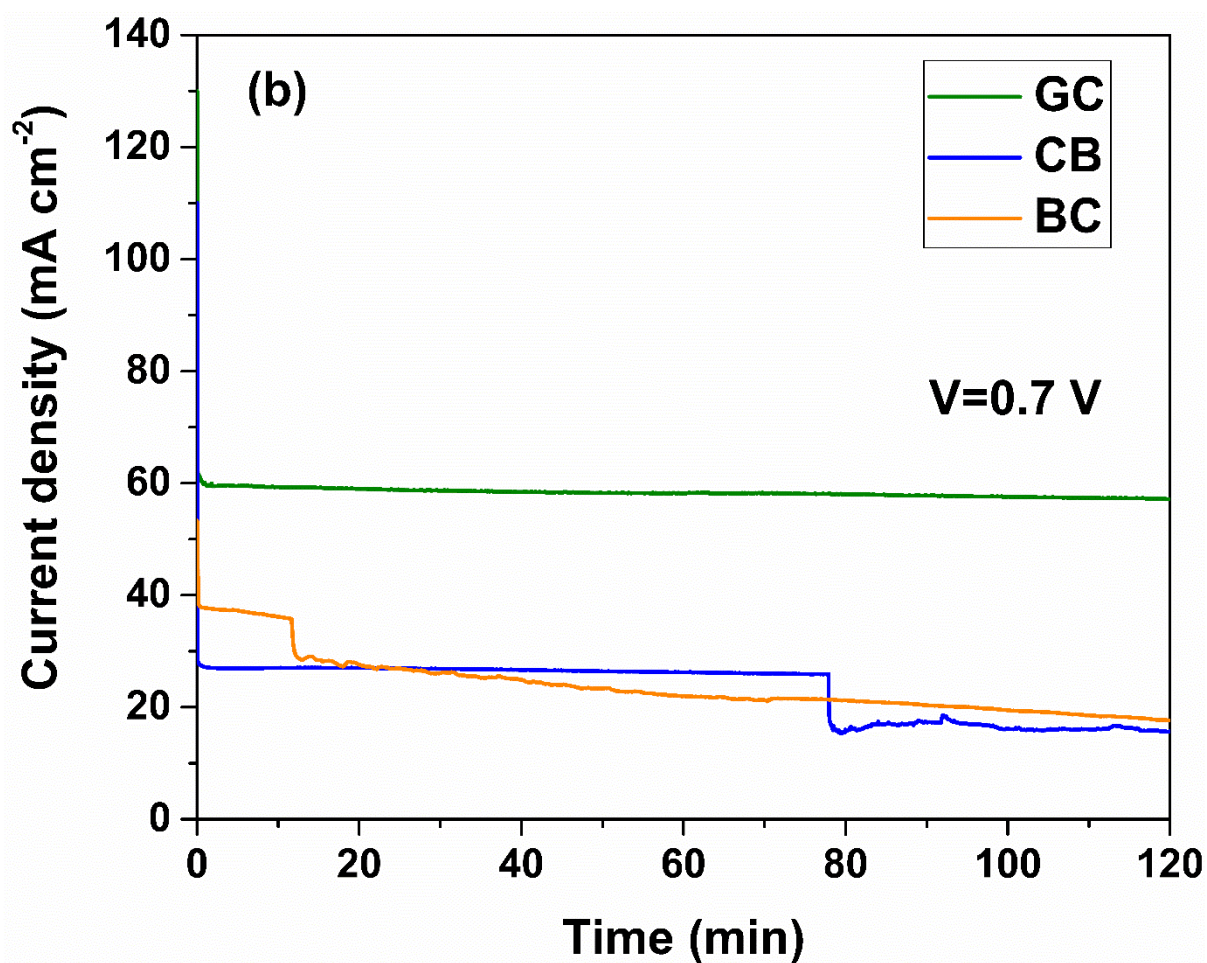
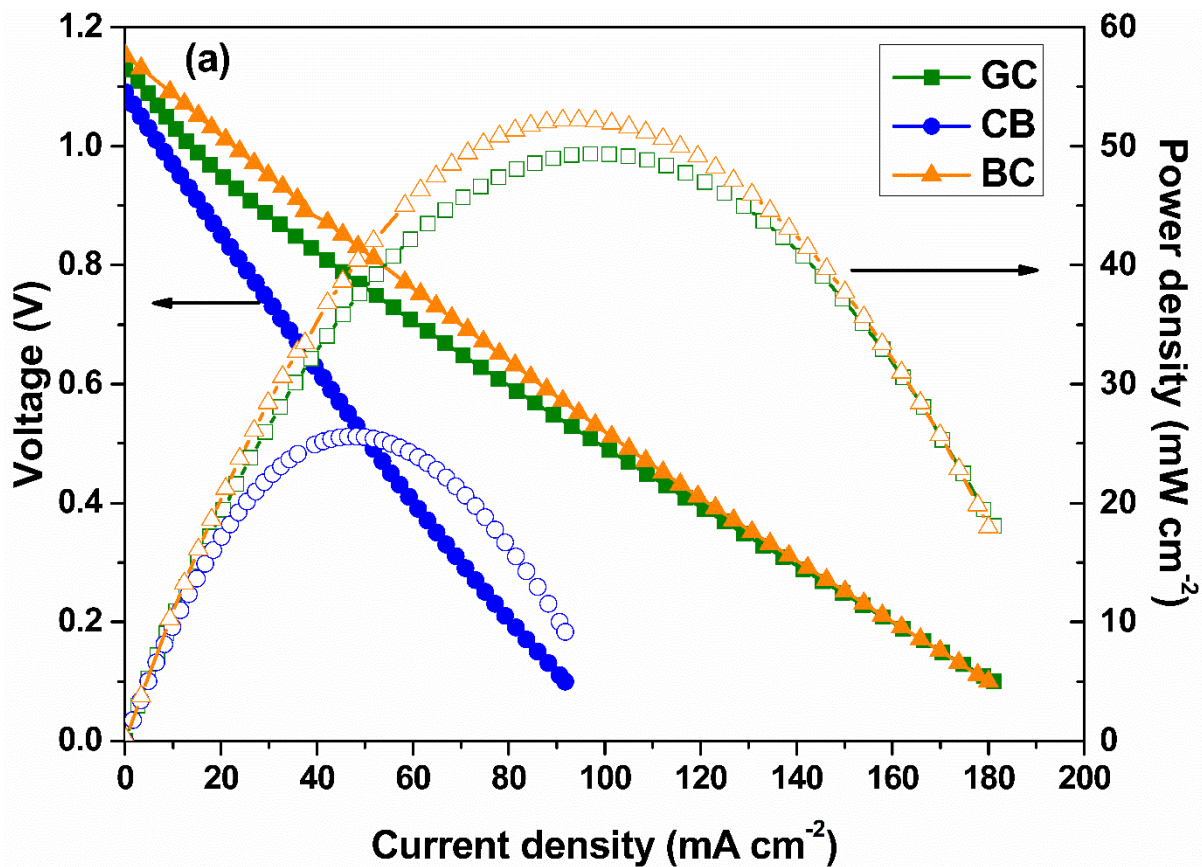
elements of carbon, hydrogen, nitrogen, and sulfur in GC, CB, or BC was analysed with CHNS element analysis (EA 1110 CHNS). The carbon powders were tested on Scanning Electron Microscope Jeol JSM-5600.

3. Results

3.1 Electrochemical performance of electrolyte-supported cells

The electrochemical reactivity of different carbon fuels was evaluated on HDCFC with a thin NiO anode. Fig.1 shows electrochemical performance of HDCFCs with GC, CB, and BC fuels. The polarisation curves of these three carbon fuels are similar in shape with linear curves presented. It demonstrates that BC produced the highest cell performance (Fig. 1a). GC-fuelled cell gave slightly lower performance than the BC-fuelled cell. The HDCFC operated with CB fuel offered the lowest performance. The maximum power density for GC fuelled HDCFC and BC fed HDCFC is 49 mW cm^{-2} and 52 mW cm^{-2} , respectively, while the maximum power density of HDCFC with CB fuel is only 25 mW cm^{-2} . Although BC and GC generate similar initial cell performance, these two fuels seem to differ regarding cell durability. Fig. 1b, which shows the current density recorded under a constant load for each fuel, indeed indicates that the cell using GC shows the best stability. The AC impedance spectra in Fig. 1c confirm these results, smaller resistance obtained on the HDCFC with BC and GC fuels, but larger resistance value when carbon black as the fuel.

The open circuit voltages of the cells with three different carbon fuels are slightly different. CB presents the low OCV value, which is 1.09 V, and the other two carbon fuels give somewhat higher voltages of 1.13 V and 1.15 V for GC and BC, respectively.



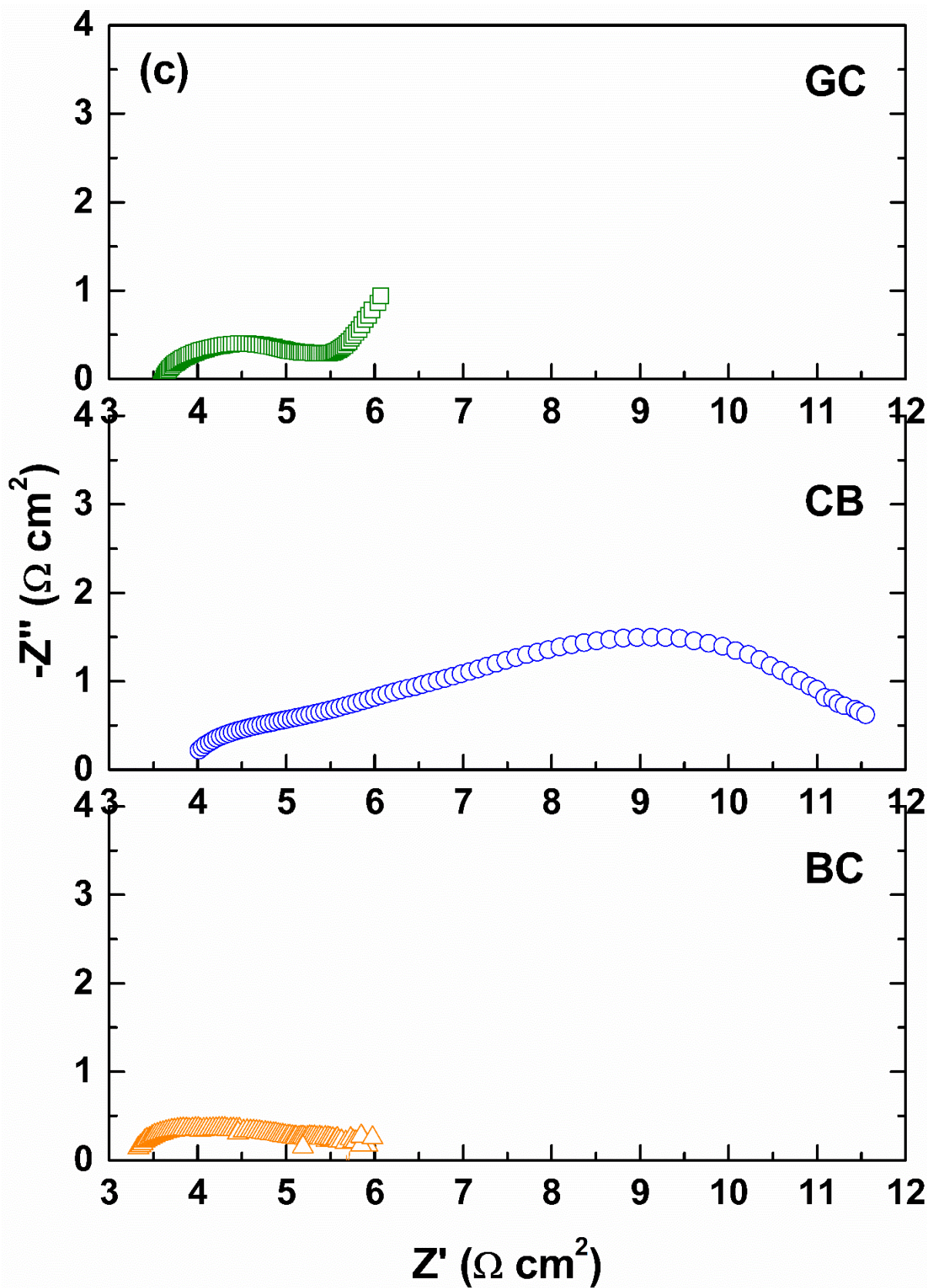


Fig. 1 Electrochemical performance of the electrolyte-supported HDCFCs with GC, CB or BC as the fuel. (a) I-V-P curves; (b) Durability of the cell under 0.7 V potential; (c) Ac impedance spectra.

3.2 Properties of fuels

To evaluate the possible dominant impact on the HDCFC performance, fuels used in this article are characterised on crystal structure, particle size, impurities and surface properties of the fuels.

Crystallinity

The DCFC performance may be dominated by structure, such as the graphitisation or surface properties. Amorphous carbon, such as active carbon, was reported easier to convert electrochemically due to the many types of reaction site (an edge, step, or other surface imperfection) for carbon oxidation [20]. Nurnberger [30] and Kulkarni [31] reported that amorphous carbon black was more reactive than graphitic carbon in DCFCs, which utilised a solid oxide electrolyte. Nurnberger *et al.*[30] developed a direct contact method to convert the chemical energy of Vulcan XC72R and GC (GFG 50M) into electricity. Their results show that Vulcan XC72R fuel generates a better performance compared to the cell with GC. The higher activity of amorphous carbon has been reported as well for molten carbonate electrolytes [20].

Carbon fuels with a typical crystal structure are chosen for investigation. CB and BC belong to amorphous carbon, but the former is pure carbon, the latter has impurities except for carbon. Fig. 2 shows the XRD patterns of GC, CB, and BC. It can be observed that an intense peak of 26.5° is the (002) graphitic basal plane reflection. Both of CB and BC have a broad diffraction peak at 23.44° , which is also (002) reflection. Another broad peak at 43.05° is the (001) GC crystal faces reflection in each pattern of carbon black and BC. These diffraction patterns confirm that carbon black and BC have amorphous structures while GC is ordered.

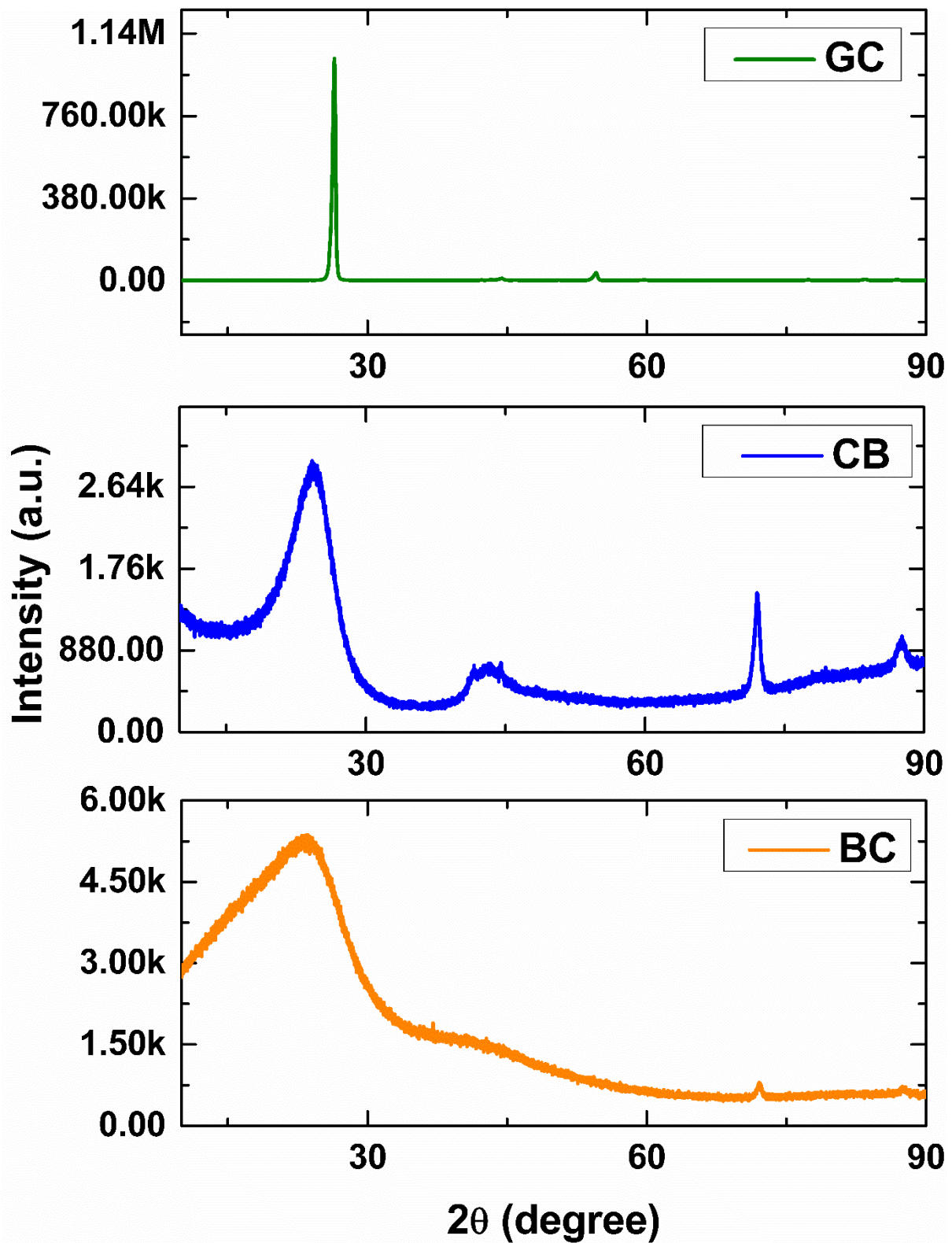


Fig. 2 XRD patterns of GC, CB and BC

Particle size

The primary particle size of the solid carbon is one parameter determining DCFC performance. In Vutetakis initial experiment, the current density of the cell increased as the particle size of coal

decreased in molten carbonate slurry under 100% CO₂ gas at 700 °C[24]. Lee *et al.* [32] also found a similar trend in SOFC mode for direct carbon oxidation. They found there is an influence of the GC particle size on the open-circuit voltage of tubular cells. It showed that the direct carbon fuel cell with the smallest particles size (32 μm) coal exhibited the highest open-circuit voltage (OCV) in the temperature range from 200 °C to 1000 °C. We had found the similar results of the influence of particle size on the OCV. CB has the smallest particle size and therefore gave the highest OCV value of 1.15 V (Fig. 1a), while BC has the biggest particle size among there carbon fuels so that the lowest OCV value of 1.09 V (Fig. 1a) was obtained. The higher OCV could be explained by the increased number of available active sites implying a higher chemical activity of the fuel.

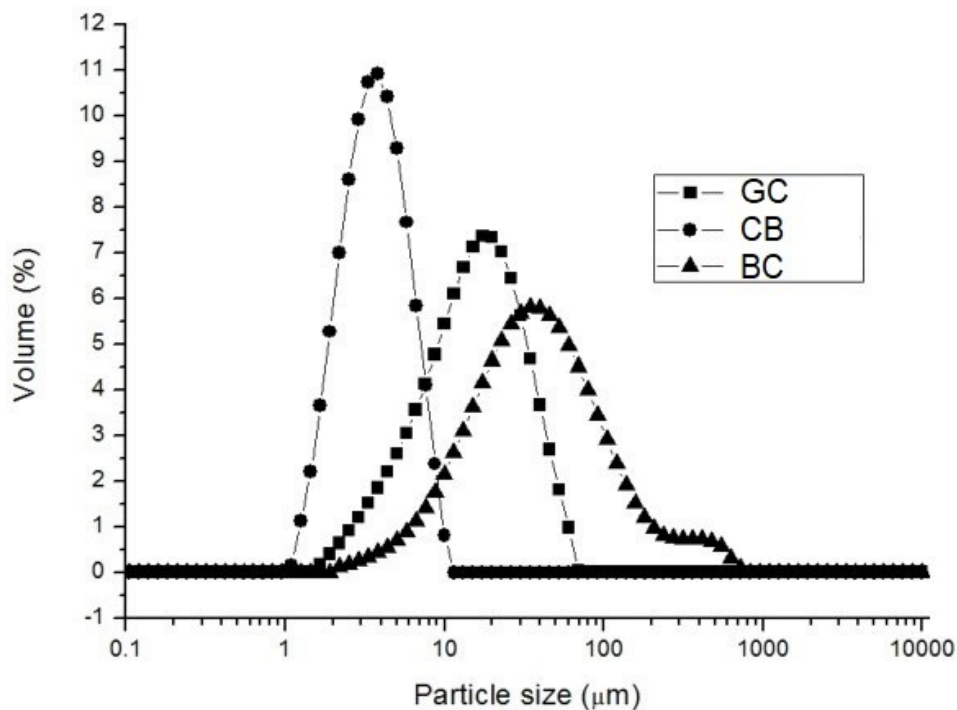
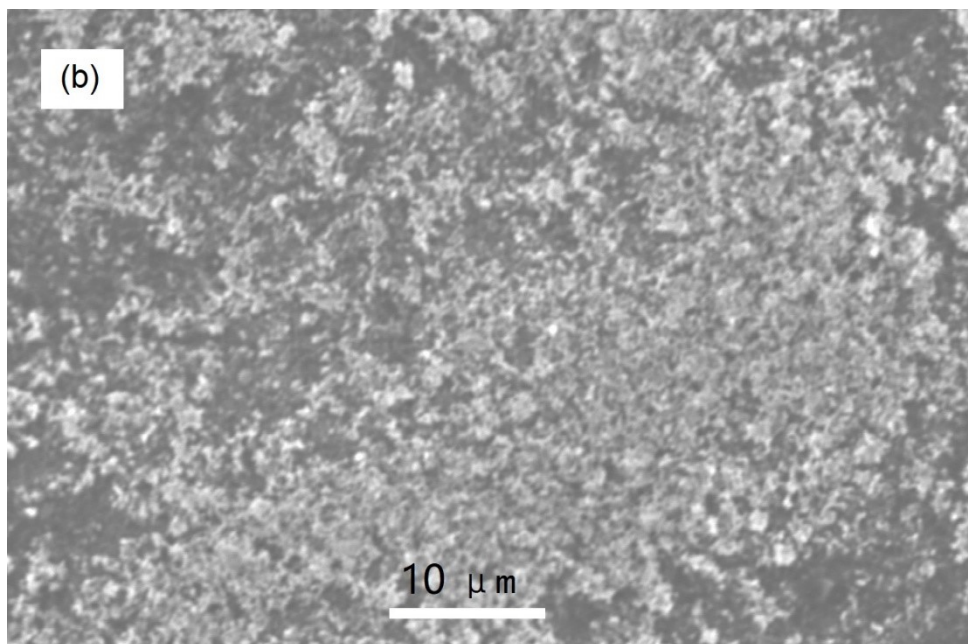
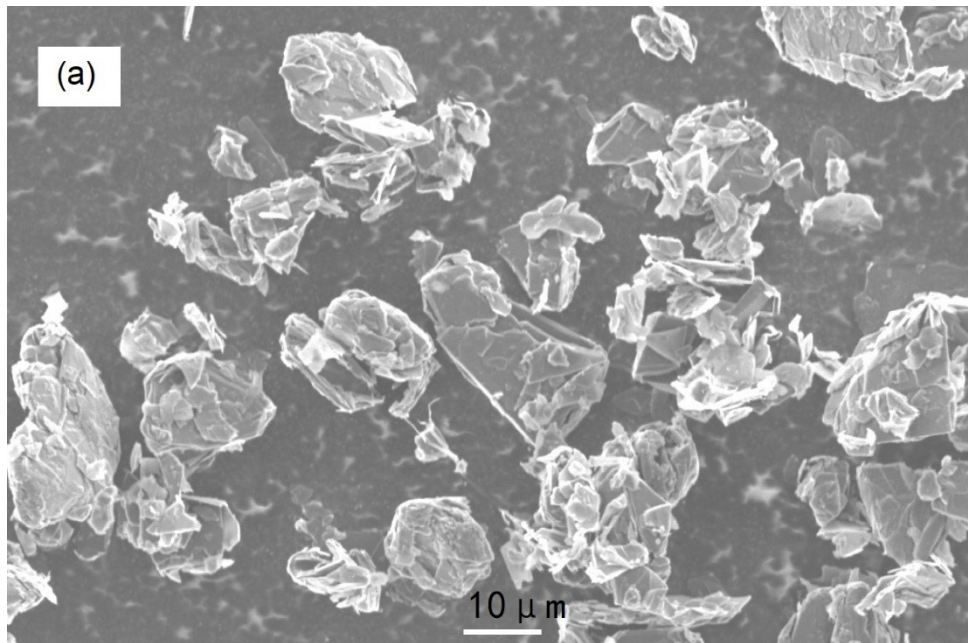


Fig. 3 Particle size and distribution of GC, CB and BC

Fig. 3 and Fig. 4 show the particle size of tested carbon fuels and SEM picture of each carbon, respectively. CB has the smallest particle size and also, of course, a large surface area (250 m²/g). The particle size of BC is big, and it also can be seen from Fig. 3 that the particle size distribution has two ranges, and some big particles exist in the range of 200 μm to 1000 μm. GC's particle size is not big, and the average size is 20 μm. The result shows that carbon with a small surface area performs better than carbon with a large surface area, which could be explained by the low reacting ability of low surface

area carbon. And also, part of the fuel will be lost by the gasification process instead of being oxidised electrochemically, therefore lower utilisation will be obtained.



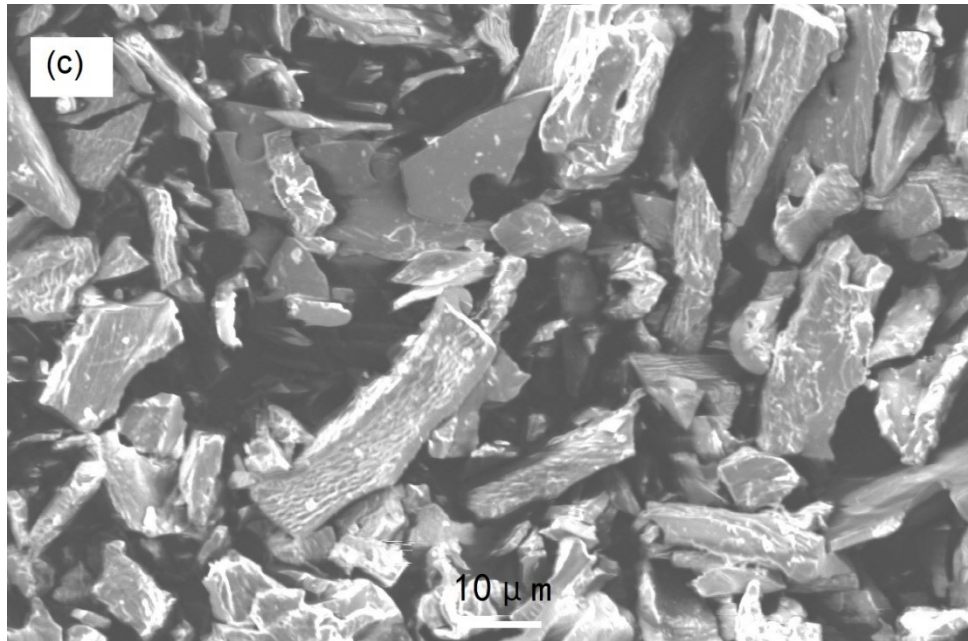


Fig. 4 SEM images of GC, CB and BC fuel

Composition

In some carbon fuels such as biomass-derived chars and coals, species containing hydrogen, oxygen, nitrogen, and sulfur may also be involved in the electrochemical process. Coal and biomass carbons contain variable amounts of non-carbon species such as tars [33]. These species might be able to improve cell performance as well as more natural activation. In impure carbon, the high-temperature pyrolysis products such as hydrogen and methane can be oxidised and so that electricity is generated. Sulfur in coal is harmful to the cell power output if nickel is used for the catalyst because it is sensitive to the presence of sulfur.

GC and CB are commercial samples. Among them, GC has high purity with 0.01% nitrogen. There are 0.09% nitrogen in CB, and some oxygen presents as well, while BC has a much lower carbon content, which is only 70.4%. The other elements like hydrogen, nitrogen is 3.5% and 4.6% respectively. There is a significant amount of oxygen (21.5%) in BC. The high oxygen level provides a benefit to the cell initial performance as we can see BC generated the best initial performance among all three-carbon fuels. This result is in good agreement with the result that pre-oxidised coal with much high oxygen contents generated higher initial power density in the same conditions in other publication [34]. CB and BC used in this research have chemisorbed oxygen complexes (i.e., carboxylic, quinonic, lactonic, phenolic groups and other) as we can see from their high oxygen content (Table 1). These surface oxygen groups are often referred to as volatile content. The volatile matter plays an essential role in cell

performance. However, the volatile matter decomposes as a loss, and only part of the decomposition takes part in the chemical reactions before the cell is on the operation (cell's target temperature is 750 °C in here). There are 30 wt% loss from BC tested in nitrogen, while only a little loss from GC shown in TG results in our previous paper [27].

There are some other elements in BC (hydrogen, nitrogen). When using BC as fuel, the amount of each gas (hydrogen, nitrogen) from the outlet of the anode is much more than the amount of the corresponding gas in CB fuel and GC (Table 1). For coal, there are some impurities, such as Al₂O₃, SiO₂, CaO, MgO, and Fe₂O₃. Contaminants such as Al₂O₃ and SiO₂ lead to an inhibitive effect during the anodic reaction in the DCFC, while CaO, MgO and Fe₂O₃ exhibit a catalytic effect on the electrochemical oxidation of carbon[17]. There are no impurities in GC, CB, and BC, so that no inorganic impurities issue is involved in this study. Detailed research of the contaminants on the GC oxidation can be found in Tulloch's report [35].

Table 1 Element analysis of GC, CB, and BC

Element	C	H	N	S	O
GC	99.9	0.00	0.01	0.00	0.00
CB	97.02	0.00	0.09	0.00	2.89
BC	70.4	3.50	4.60	0.00	21.5

Surface properties

Fig. 5 shows the FTIR spectra of each carbon fuel. We can see from the FTIR spectra, aromatic peaks and conjugates and non-conjugates bonds are clearly visible at 1690 and 1606 cm⁻¹ for BC, while the same peaks are partially visible or absent for CB and GC. The same heights were observed by FTIR analysis, which has been found in Solum's research. The peak at 1383 cm⁻¹ is the only peak visible in all of three spectra because they characterise the methyl group as a terminal in the aromatic cluster and the intensity of these peaks can be used to determine the amount of aromatic cluster in the structure. And also, comparing three different types of carbons (GC, CB, and BC) by FTIR analysis, we can observe how the aromatic bonds and C-O peaks decrease as a function of the extent of carbon oxidation.

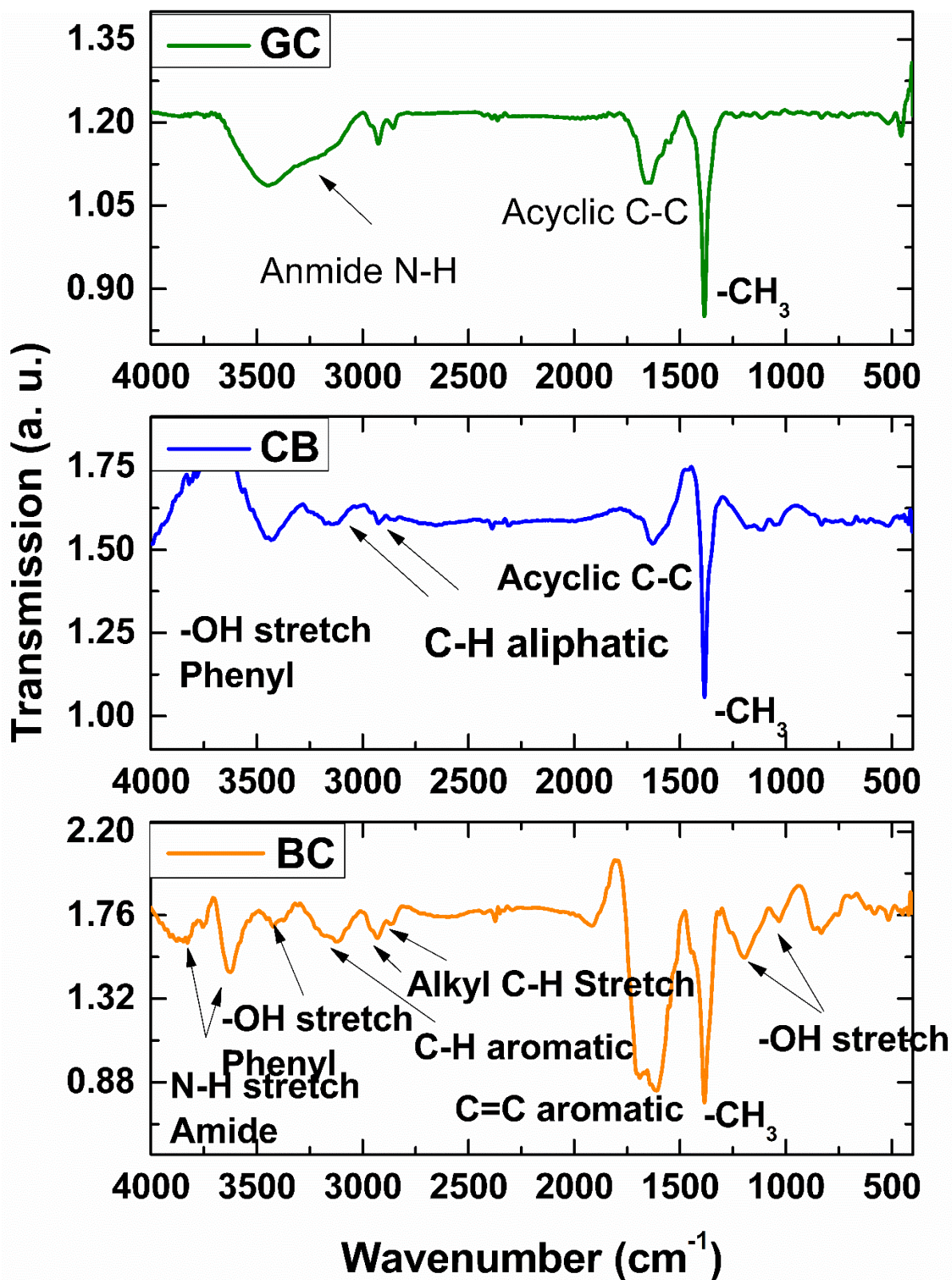


Fig. 5 FTIR spectra of GC, CB and BC

3.4 Gas products

The TPD files of DCFCs under open-circuit voltage condition using these three carbons are shown in Fig. 6. Although it is difficult to directly retrieve information about the exact type of surface functional

group, the general information on reactive surface sites can be derived from the TPD profiles. Four gases of H₂, CO, CO₂, and CH₄ were observed. During the TPD process, the surface complexes would release CO₂ and CO at different temperatures. In general, CO₂ evolves from the decomposition of carboxylic acid functionality at low temperatures and/or lactones at high temperatures, while CO arises from the phenols and carbonyls at high temperature.[36] As expected, GC produces the smallest amounts of all gases, like H₂, CO, CO₂, and CH₄ due to the greatest extent of carbon oxidation. It can be seen that there is no hydrogen (0% hydrogen from element analysis in Table 1), while more hydrogen product in the BC (3.53% hydrogen from element analysis in Table 1) fuelled cell since there are more –OH stretch and C-H aliphatic functional groups in BC. CO₂ and CO evolution from GC is nearly negligible, indicating a surface clean of oxygen complex groups, whereas BC generates the most significant amount of CO₂ with a maximum peak at around 450 °C. This result can be confirmed by the low oxygen content in GC, as shown in Table 1(no oxygen in GC). CO evolution takes place at a much higher temperature, and the height of CO evolution for BC and CB are located at 675 °C and 750 °C [37]. In addition, little methane is found between 400 to 500 °C from the off-gas, which is produced by the pyrolysis process of the carbon when CB and BC as the fuel, while no methane is observed with GC as the fuel (Fig. 6). With the temperature increasing methane reacts with water and produces hydrogen and carbon dioxide by eqn. (1).



Methane is completely consumed to produce hydrogen and carbon monoxide higher than the testing temperature of 750 °C. Carbon has a different crystal structure, and the oxidation of carbon into carbon dioxide is determined by the activation of the carbon itself. For the semi-pyrolysed carbon, it is easier to be activated since more active species or bonds to carbon and therefore much better cell performance. This product of hydrogen is helpful with the reduction of nickel oxide to nickel metal. The evolution profile of these four different gases is more likely related to the nickel reduction as there is no electrochemical reactions happens. Therefore, the cell performance with different GC is more related to the cell itself rather than the pyrolysis gases. The initial cell performance was governed primarily by the amount of hydrogen and CO released at 750 °C (as the cell performance is tested at this temperature). It must be noticed that water produced by hydrogen electrooxidation can react with carbon and generate active gases, like hydrogen and CO. Further research is necessary to evaluate the influence of this reaction on the cell performance.

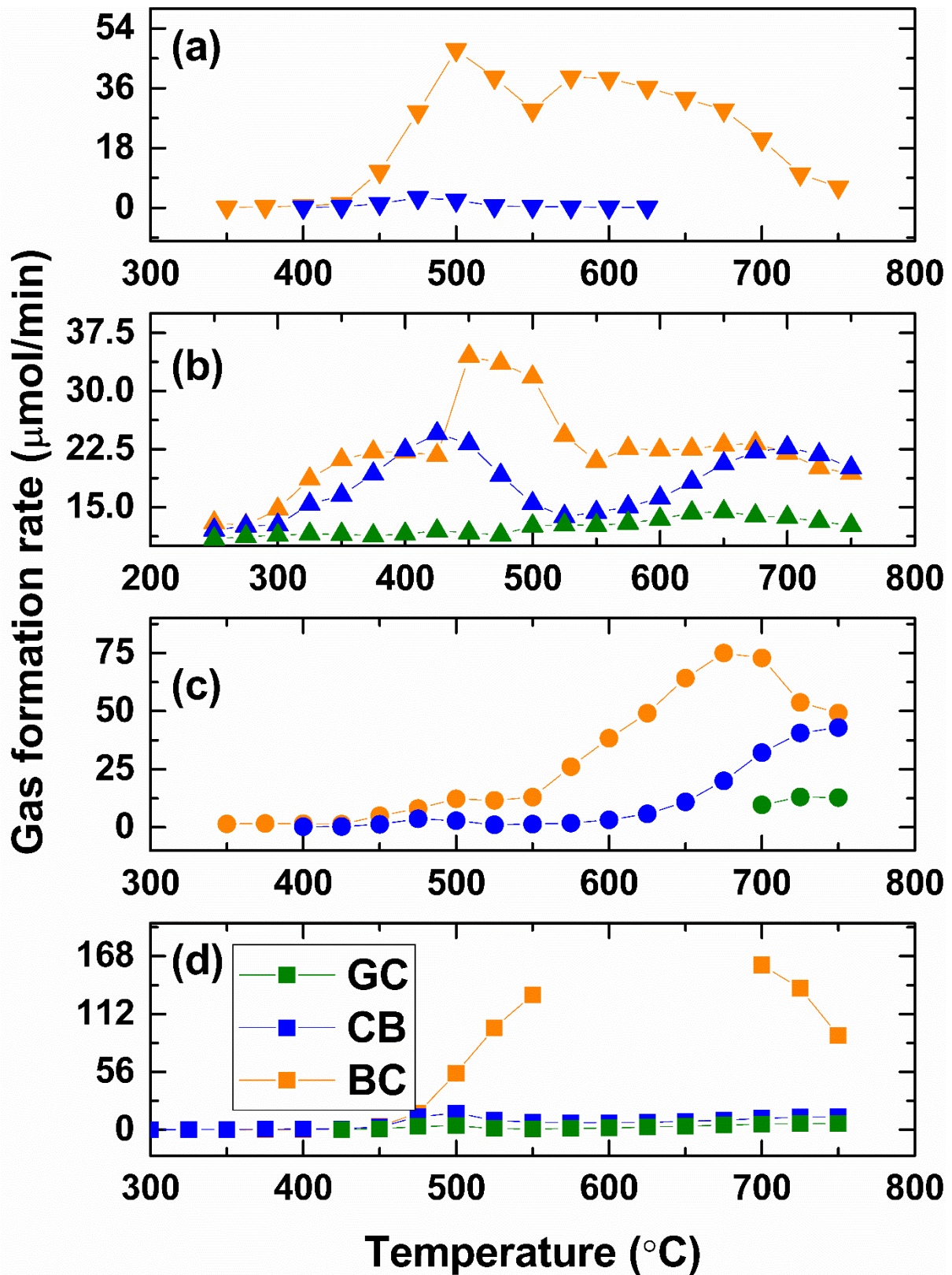


Fig. 6 Gas products of the outlet for the cells with GC, CB or BC as the fuel (Formation rate of hydrogen from BC fuel at 550 °C to 700 °C is above the limitation of GC detect). (a) CH₄; (b) CO₂; (c)CO; (d)H₂

Fig. 7 shows the gas analysis under current load (cell performance shown in Fig. 1b). It can be seen that similar amounts of CO_2 are produced for these three carbons, while there are significant differences for CO and H_2 products. In the beginning, hydrogen oxidation is the dominant process, along with carbon oxidation. With the time increase, less hydrogen left in the anode chamber as the diffusion rate of hydrogen is fast. A much lower CO formation rate for GC than CB and BC was found in the first 30 mins. After 30 mins of the durability test, a significant amount CO is produced when GC is used for the fuel, which might be because the cell performance is dominant by carbon oxidation and Boudouard reaction in the process.[37] The CO formation was due to the slow oxidation rate of GC because of its high extent of graphitisation (Fig. 2). CB and BC are amorphous and more active than GC. which has been displayed in TGA tests in our previous paper, in where the onset of oxidation temperature is around $640\text{ }^\circ\text{C}$ while that is about $540\text{ }^\circ\text{C}$ [27]. As compared to the electrochemical reaction rate of hydrogen, carbon oxidation is a slow process. Therefore, after a certain time, carbon oxidation is the dominant process. GC has the highest amount of carbon, which might be the reason that GC-fuelled direct carbon fuel cell gives better cell performance than other carbons-fuelled cells (Fig. 1a).

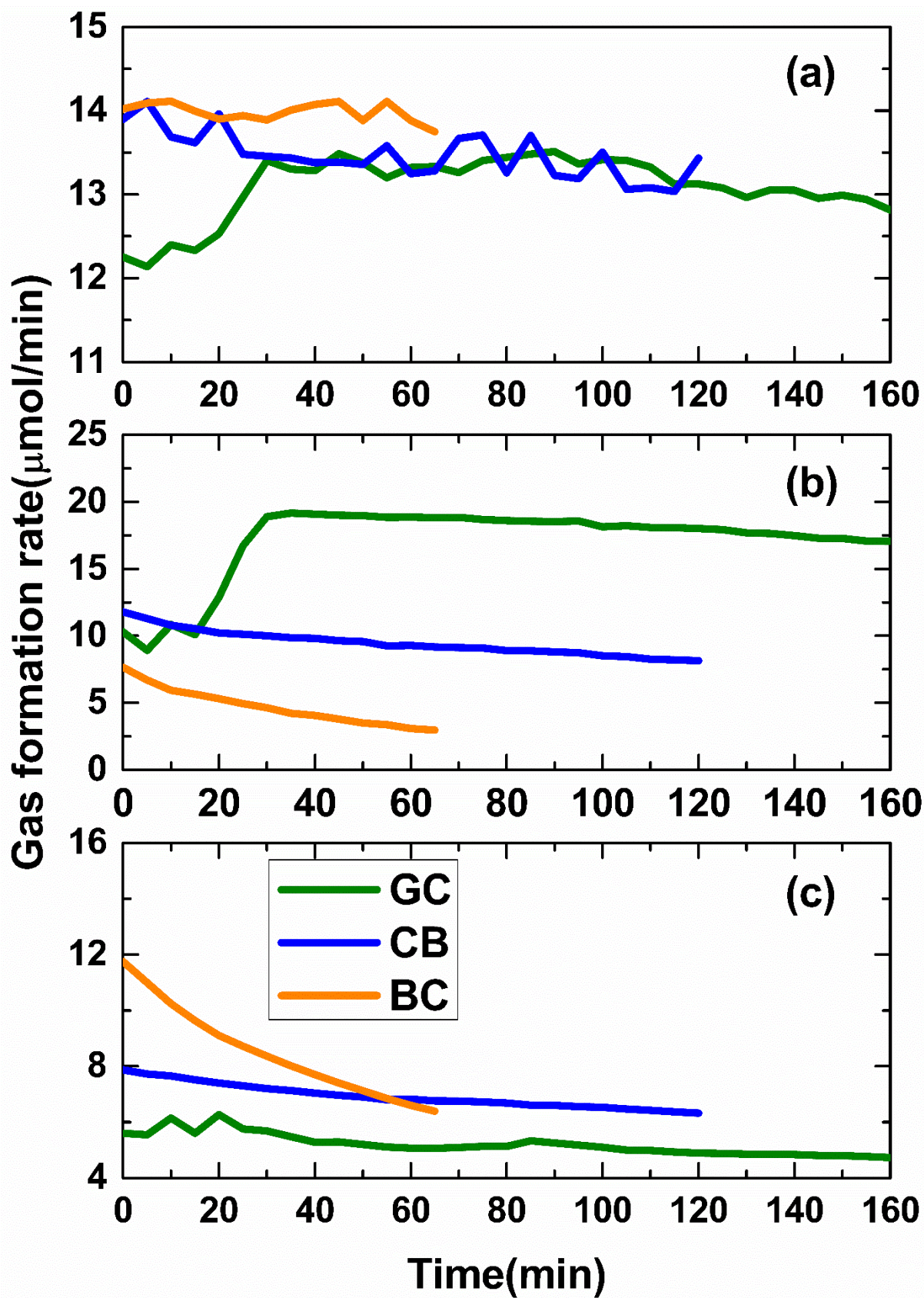
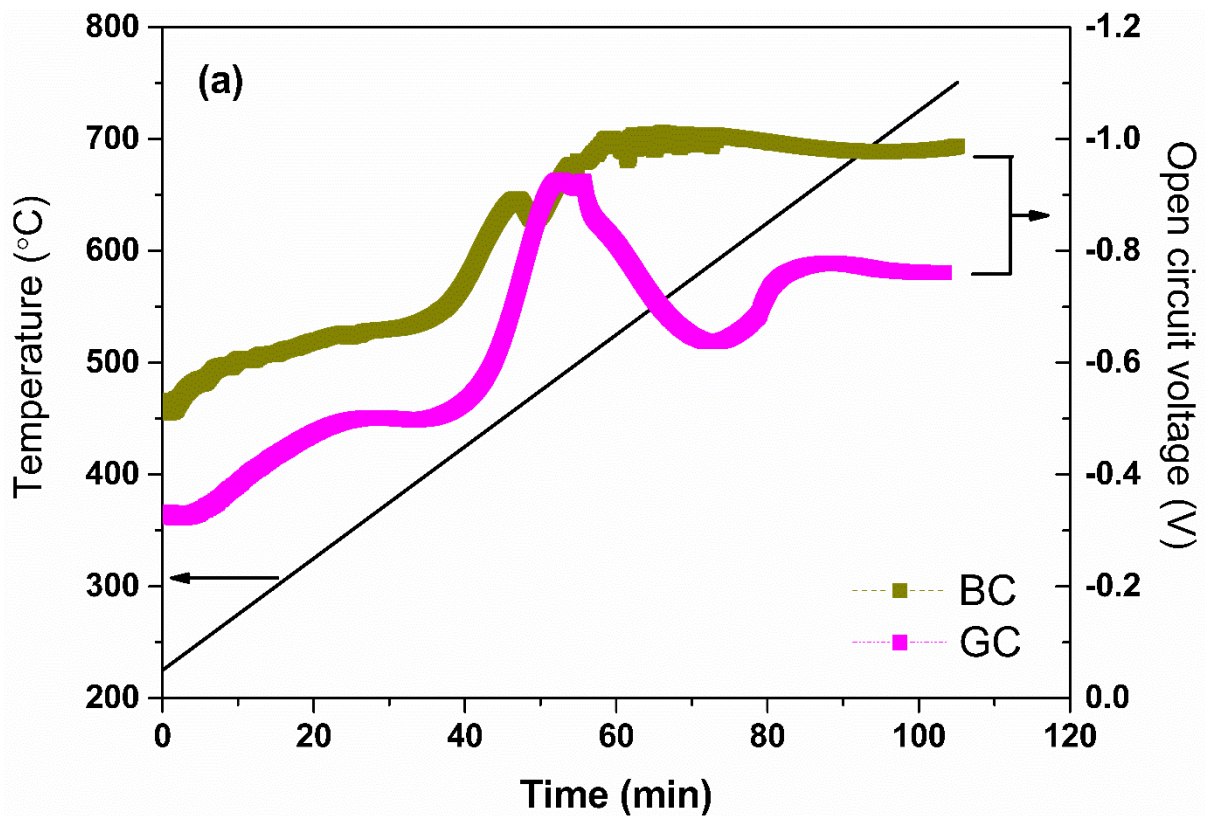
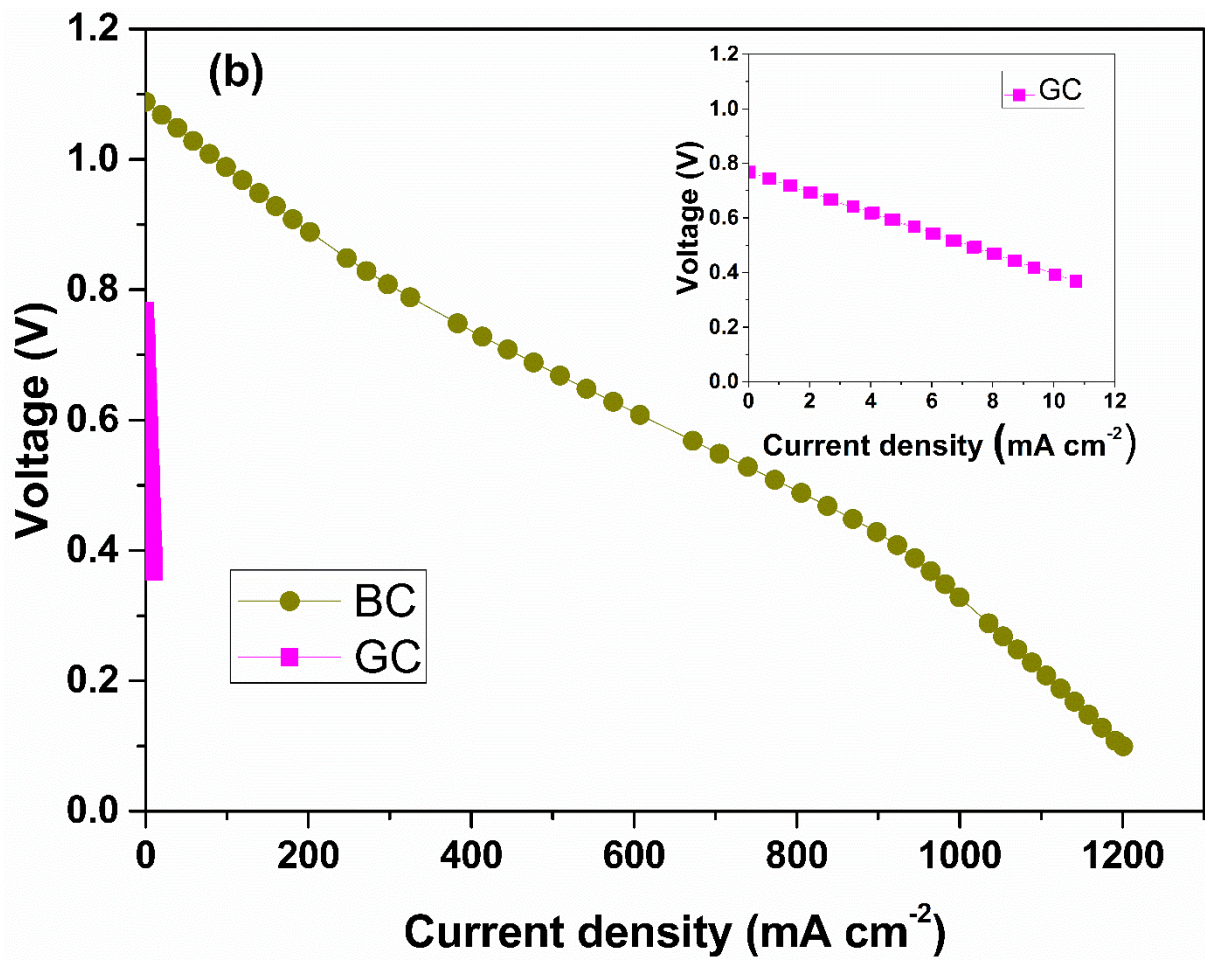


Fig. 7 Gas analysis of the HDCFC operating at 0.7 V using GC, CB or BC as the fuel. (a) CO₂; (b) CO;
(c) H₂

3.5 HDCFC performance on a thick NiO anode

HDCFC performance was investigated on thick NiO anodes using these three carbon fuels. The open-circuit voltage was recorded when the HDCFC was heating up to the operating temperature of 750 °C. The cell OCV increases with the increase in temperature using CB and GC fuels. NiO is reduced when the temperature is higher than 500 °C. It can be seen from Fig. 8a, CB fuelled HDCFC is reduced so fast, while it takes a much longer time for GC fuelled HDCFC to be reduced. It is not even fully reduced when the cell reached to the test temperature of 750 °C, and the OCV is only 0.75 V. The initial cell performance of the GC-fuelled DCFC is much lower than the CB-fuelled DCFC (Fig. 8b). The cell is reduced when it is operating at 750 °C for 10 hours, and the cell performance is improving with time (Fig. 8c).





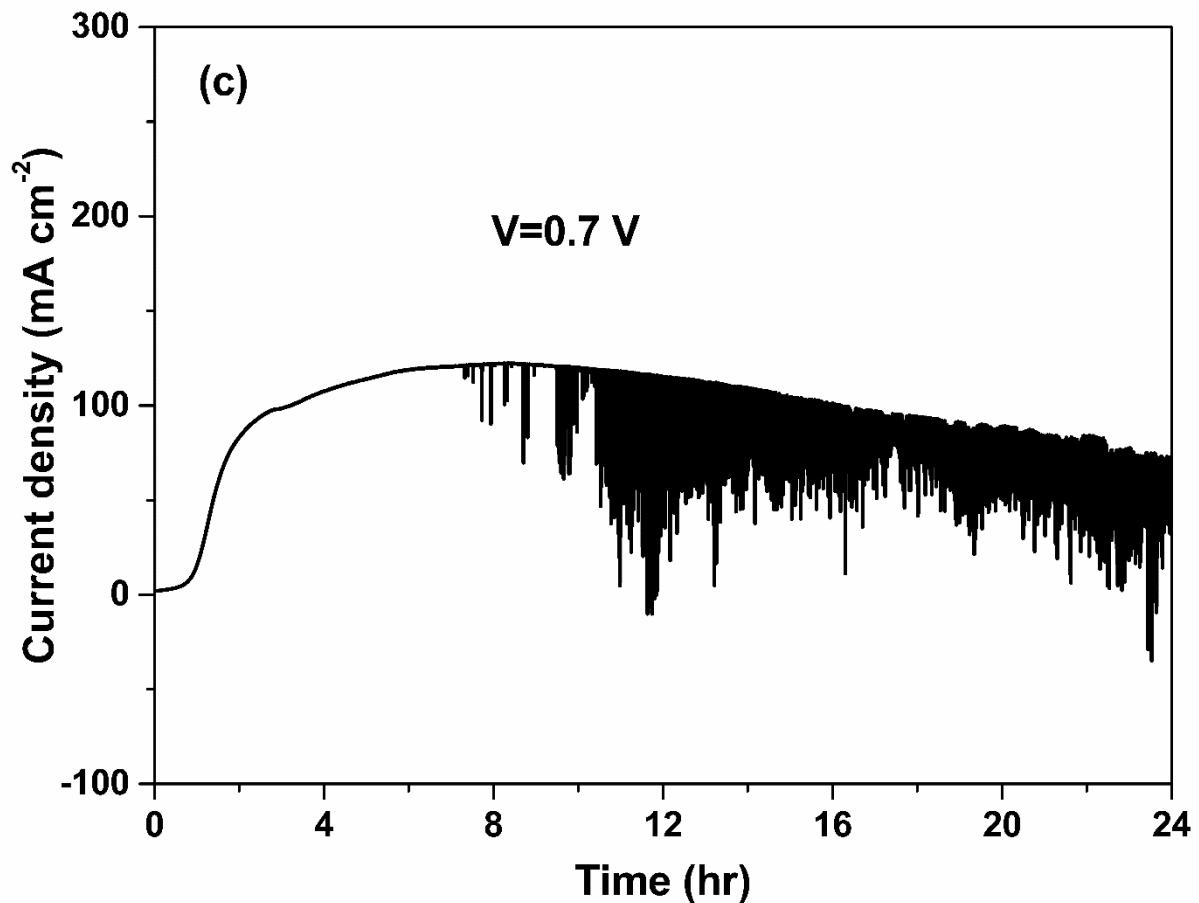


Fig. 8 Electrochemical performance of a NiO-anode supported cell with a configuration of 1 mm thick NiO anode/ thin YSZ electrolyte/ $(\text{La}_{0.8}\text{Sr}_{0.2})_{0.95}\text{MnO}_{3-\delta}$ /YSZ composite cathode, using GC or BC as a fuel. (a) Open circuit voltage of HDCFC with time during the cell is heating up to 750°C; (b) I-V curves of HDCFC operating at 750°C with GC or CB as the fuel; (c) Long-term stability of HDCFC tested at 750°C with GC as the fuel

Fig. 9 displays the formation rate of carbon monoxide at different voltage loads tested at 750 °C. It can be seen that the CO formation rate decreases with the voltage load. The high CO content shows that it is desirable of partially carbon oxidation at high current (low voltage) with more products of CO.

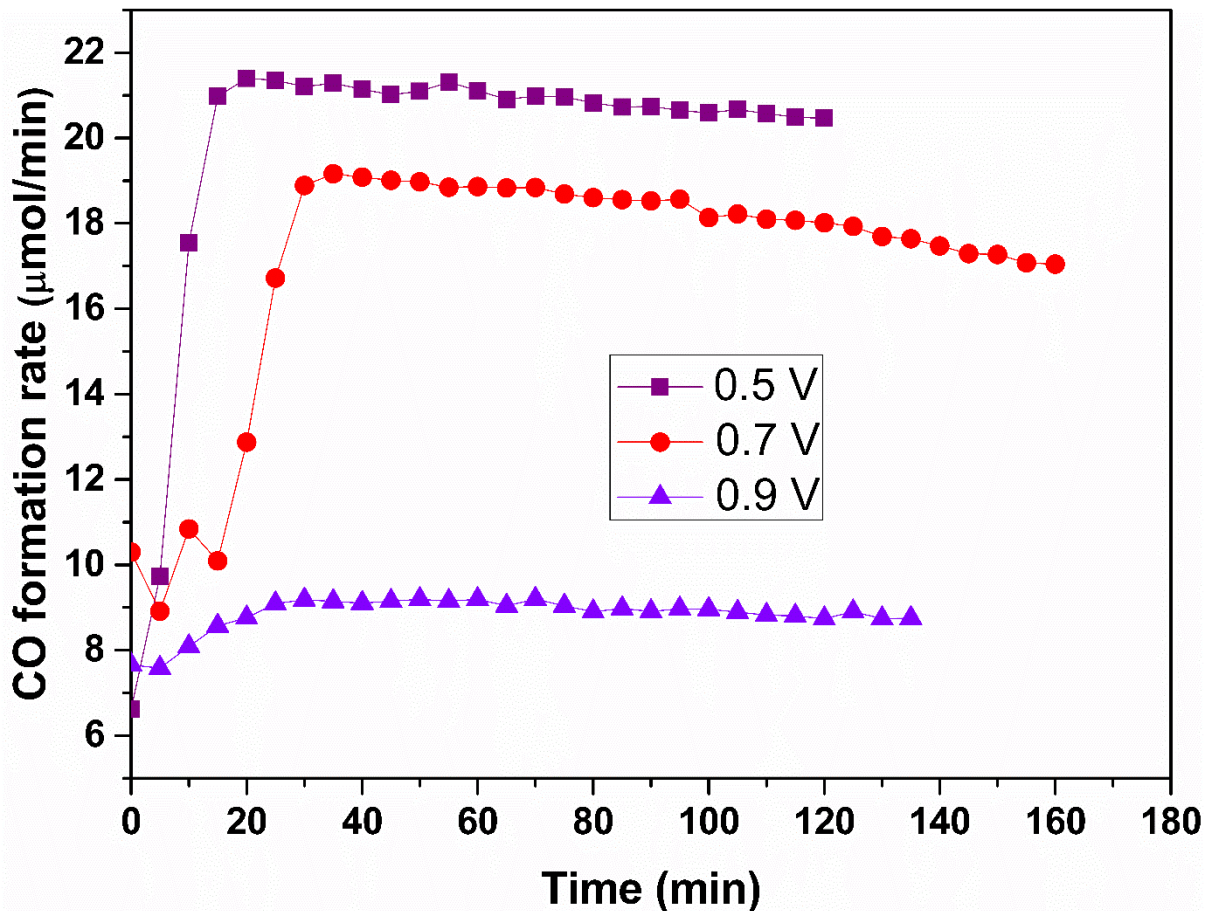


Fig. 9 CO formation of the HDCFC with a configuration of 1 mm thick NiO anode/ thin YSZ electrolyte/ $(\text{La}_{0.8}\text{Sr}_{0.2})_{0.95}\text{MnO}_{3-\delta}$ /YSZ composite cathode, operating at different voltage loads with GC as the fuel

4. Conclusion

The electrochemical reactivity of carbon fuels on nickel oxide-based hybrid direct carbon fuel cells (HDCFCs) is investigated. Graphite (GC), carbon black (CB), and biomass carbon (BC) fuels were chosen as the fuel. GC generated good initial cell performance and long-term stability on the electrolyte-supported HDCFC. It suggested that the HDCFC performance is affected by composition and surface property, and is less likely to be dependent on the particle size and the crystal structure when using thin nickel oxide anode. However, GC showed the worst cell performance and reasonable durability on the anode-supported cell, indicating that the reactivity of carbon on anode-supported is possibly related to the crystal structure, composition, and surface property. TPD files of the HDCFCs show that H_2 and CO are the two main gases. In-situ gas analysis under voltage load showed that hydrogen oxidation contributed partially to the cell performance, and however after a certain time when the hydrogen is not the dominant composition, carbon oxidation is the dominant process with CO released probably

because of the Boudourad reaction. This study demonstrates attractive attributes of the mechanism insight of carbon oxidation by in-situ gas analysis, suggesting that GC is a potential fuel for hybrid direct carbon fuel cells.

Acknowledgement

This work was supported by Sichuan Science and Technology Program (grant number 2019YFH0177); the talent introduction plan of Sichuan University of Science and Engineering (grant numbers 2016RCL36, 2016RCL37); enterprise cooperation project (grant number HX2017087); and the opening project of Material Corrosion and Protection Key Laboratory of Sichuan Province (grant numbers 2017CL11 and 2017CL13). CJ acknowledges the Royal Society of Edinburgh for an RSE BP Hutton Prize in Energy Innovation.

References

- [1]Wu W, Zhang Y Y, Ding D, He T. A High-Performing Direct Carbon Fuel Cell with a 3D Architected Anode Operated Below 600 degrees C. *Adv Mater* 2018; 30: 6.
- [2]Rady A C, Giddey S, Kulkarni A, Badwal S P S, Bhattacharya S, Ladewig B P. Direct carbon fuel cell operation on brown coal. *Appl Energ* 2014; 120: 56-64.
- [3]Jiang C, Ma J, Corre G, Jain S L, Irvine J T S. Challenges in developing direct carbon fuel cells. *Chem Soc Rev* 2017; 46: 2889-912.
- [4]Zhang J B, Zhong Z P, Zhao J X, Yang M, Li W L, Zhang H Y. Study on the preparation of activated carbon for direct carbon fuel cell with oak sawdust. *Can J Chem Eng* 2012; 90: 762-8.
- [5]Nabae Y, Pointon K D, Irvine J T S. Ni/C Slurries Based on Molten Carbonates as a Fuel for Hybrid Direct Carbon Fuel Cells. *J Electrochem Soc* 2009; 156: B716-B20.
- [6]Li X, Zhu Z H, Chen J L, De Marco R, Dicks A, Bradley J, et al. Surface modification of carbon fuels for direct carbon fuel cells. *J Power Sources* 2009; 186: 1-9.
- [7]Jain S L, Nabae Y, Lakeman B J, Pointon K D, Irvine J T S. Solid state electrochemistry of direct carbon/air fuel cells. *Solid State Ionics* 2008; 179: 1417-21.
- [8]Liu R Z, Zhao C H, Li J L, Zeng F R, Wang S R, Wen T L, et al. A novel direct carbon fuel cell by approach of tubular solid oxide fuel cells. *J Power Sources* 2010; 195: 480-2.
- [9]Guo L, Calo J M, Dicocco E, Bain E J. Development of a Low Temperature, Molten Hydroxide Direct Carbon Fuel Cell. *Energ Fuel* 2013; 27: 1712-9.

- [10]Lee E K, Park S A, Jung H W, Kim Y T. Performance enhancement of molten carbonate-based direct carbon fuel cell (MC-DCFC) via adding mixed ionic-electronic conductors into Ni anode catalyst layer. *J Power Sources* 2018; 386: 28-33.
- [11]Fini D, Badwal S P S, Giddey S, Kulkarni A P, Bhattacharya S. Evaluation of $\text{Sc}_2\text{O}_3\text{-CeO}_2\text{-ZrO}_2$ electrolyte-based tubular fuel cells using activated charcoal and hydrogen fuels. *Electrochim Acta* 2018; 259: 143-50.
- [12]Hackett G A, Zondlo J W, Svensson R. Evaluation of carbon materials for use in a direct carbon fuel cell. *J Power Sources* 2007; 168: 111-8.
- [13]Weaver R D, Leach S C, Bayce A E, Nanis L. Direct Electrochemical Generation of Electricity from Coal. Quarterly progress report No. 2 (Monthly progress report No. 6). United States: N. p., 1976. Web.
- [14]Ahn S Y, Eom S Y, Rhie Y H, Sung Y M, Moon C E, Choi G M, et al. Application of refuse fuels in a direct carbon fuel cell system. *Energy* 2013; 51: 447-56.
- [15]Chen C-C, Maruyama T, Hsieh P-H, Selman J R. The Reverse Boudouard Reaction in Direct Carbon Fuel Cells. *Ecs Transactions* 2010; 28: 227-39.
- [16]Peng F, Li Y, Nash P, Cooper J F, Parulekar S J, Selman J R. Direct Carbon Fuel Cells - Wetting behavior of graphitic carbon in molten carbonate. *Int J Hydrogen Energy* 2016; 41: 18858-71.
- [17]Li X, Zhu Z H, De Marco R, Bradley J, Dicks A. Evaluation of raw coals as fuels for direct carbon fuel cells. *J Power Sources* 2010; 195: 4051-8.
- [18]Li X, Zhu Z H, De Marco R, Dicks A, Bradley J, Liu S M, et al. Factors That Determine the Performance of Carbon Fuels in the Direct Carbon Fuel Cell. *Industrial & Engineering Chemistry Research* 2008; 47: 9670-7.
- [19]Ahn S Y, Eom S Y, Rhie Y H, Sung Y M, Moon C E, Choi G M, et al. Utilization of wood biomass char in a direct carbon fuel cell (DCFC) system. *Appl Energy* 2013; 105: 207-16.
- [20]Cherepy N J, Krueger R, Fiet K J, Jankowski A F, Cooper J F. Direct conversion of carbon fuels in a molten carbonate fuel cell. *J Electrochem Soc* 2005; 152: A80-A7.
- [21]Dudek M, Tomczyk P, Socha R, Hamaguchi M. Use of ash-free "Hyper-coal" as a fuel for a direct carbon fuel cell with solid oxide electrolyte. *Int J Hydrogen Energy* 2014; 39: 12386-94.
- [22]Elleuch A, Boussetta A, Halouani K, Li Y. Experimental investigation of Direct Carbon Fuel Cell fueled by almond shell biochar: Part II. Improvement of cell stability and performance by a three-layer planar configuration. *Int J Hydrogen Energy* 2013; 38: 16605-14.

- [23]Jewulski J, Skrzypkiewicz M, Struzik M, Lubarska-Radziejewska I. Lignite as a fuel for direct carbon fuel cell system. *Int J Hydrogen Energy* 2014; 39: 21778-85.
- [24]Vutetakis D G, Skidmore D R, Byker H J. Electrochemical Oxidation of Molten Carbonate-Coal Slurries. *J Electrochem Soc* 1987; 134: 3027-35.
- [25]Chen M M, Wang C Y, Niu X M, Zhao S, Tang J, Zhu B. Carbon anode in direct carbon fuel cell. *Int J Hydrogen Energy* 2010; 35: 2732-6.
- [26]Jiang C R, Irvine J T S. Catalysis and oxidation of carbon in a hybrid direct carbon fuel cell. *J Power Sources* 2011; 196: 7318-22.
- [27]Li S B, Pan W Z, Wang S R, Meng X, Jiang C R, Irvine J T S. Electrochemical performance of different carbon fuels on a hybrid direct carbon fuel cell. *Int J Hydrogen Energy* 2017; 42: 16279-87.
- [28]Jiang C R, Ma J J, Bonaccorso A D, Irvine J T S. Demonstration of high power, direct conversion of waste-derived carbon in a hybrid direct carbon fuel cell. *Energy Environ Sci* 2012; 5: 6973-80.
- [29]Bonaccorso A D, Irvine J T S. Development of tubular hybrid direct carbon fuel cell. *Int J Hydrogen Energy* 2012; 37: 19337-44.
- [30]Nurnberger S, Bussar R, Desclaux P, Franke B, Rzepka M, Stimming U. Direct carbon conversion in a SOFC-system with a non-porous anode. *Energy Environ Sci* 2010; 3: 150-3.
- [31]Kulkarni A, Giddey S, Badwal S P S. Electrochemical performance of ceria-gadolinia electrolyte based direct carbon fuel cells. *Solid State Ionics* 2011; 194: 46-52.
- [32]Kim J-P, Lim H, Jeon C-H, Change Y-J, Kohm K-N, Choi S-M, et al. Performance evaluation of tubular fuel cells fuelled by pulverized graphite. *J Power Sources* 2010; 195: 7568-73.
- [33]Kivisaari T, Bjornbom P, Sylwan C, Jacquinet B, Jansen D, De Groot A. The feasibility of a coal gasifier combined with a high-temperature fuel cell. *Chem Eng J* 2004; 100: 167-80.
- [34]Fuente-Cuesta A, Jiang C, Arenillas A, Irvine J T S. Role of coal characteristics in the electrochemical behaviour of hybrid direct carbon fuel cells. *Energy Environ Sci* 2016; 9: 2868-80.
- [35]Tulloch J, Allen J, Wibberley L, Donne S. Influence of selected coal contaminants on graphitic carbon electro-oxidation for application to the direct carbon fuel cell. *J Power Sources* 2014; 260: 140-9.
- [36]Zhu Z H, Radovic L R, Lu G Q. Effects of acid treatments of carbon on N₂O and NO reduction by carbon-supported copper catalysts. *Carbon* 2000; 38: 451.

[37]Xu K, Chen C, Liu H, Tian Y, Li X, Yao H. Effect of coal based pyrolysis gases on the performance of solid oxide direct carbon fuel cells. *Int J Hydrogen Energy* 2014; 39: 17845-51.